AIAA JOURNAL
Vol. 34, No. 9, September 1996

Optimum Placement of Piezoelectric Sensor/Actuator for Vibration Control of Laminated Beams

Young Kyu Kang,* Hyun Chul Park,† Woonbong Hwang,‡ and Kyung Seop Han§
Pohang University of Science and Technology, Pohang, Kyungbuk 790-784, Republic of Korea

The optimum placement of a collocated piezoelectric sensor/actuator is investigated numerically and verified experimentally for vibration control of laminated composite beams. The finite element method is used for the analysis of dynamic characteristics of the laminated composite beams with the piezoceramic sensor/actuator. The damping and the stiffness of the adhesive layer and the piezoceramics are taken into account in the process of finite element modeling. Tailoring that varies the stiffness and the damping properties of the composite material is used. The stacking sequence of the laminated composite beam is $[\theta_4/0_2/90_2]_s$, where $\theta = 0, 15, 30, 45, 60, 75,$ and 90 deg. The sensor/actuator attached to a structure changes the mass, the damping, and the stiffness of the entire structure. Thus, interaction between sensor/actuator and structure is very important in the vibration control of a flexible structure. Modal damping ($2\zeta\omega$) is chosen as a more appropriate performance index, because it is directly related to the settling time of the vibration. The structural damping index (SDI) is defined from the modal damping. Weights for each vibrational mode are taken into account in the SDI calculation. The optimum location of the sensor/actuator is determined as the point where the SDI is maximum. Numerical simulation and experimental results show that the SDI depends on outer-layer fiber orientations of the host structure, the location, and the size of the sensor/actuator.

Introduction

PIEZOELECTRIC sensors/actuators have been widely used in structural vibration control. In the case of piezoceramics, depending on the applied voltage to the piezoceramics, the electromechanical coupling of the forcing transducer to the structure, and the location of the piezoelectric transducers, a degree of vibration control of flexible structures can be considered. Because proper selection of number and location of the piezoelectric sensors/actuators is critical to control structural vibration efficiently, determining the optimum placement of piezoelectric sensors/actuators for vibration control is one of the key issues to address. To select sensor/actuator locations to control flexible structural systems, several concepts pertaining to the degree of controllability/observability and cost analysis have been developed.[1,2] These methods are shown to yield less effective results for vibration damping in structures because their concepts are focused on stiffness.

Several studies regarding placement of the actuators for vibration and acoustic control are available.[3–7] A common feature of all of these studies is ignorance of the inherent damping of the structure when using piezoelectric sensors/actuators in the formulation. When a piezoelectric sensor is used as a strain-rate sensor, the piezoelectric actuator increases the damping of the entire system. Therefore, the damping must be taken into account in the formulation of optimal placement of the sensor/actuator. Most research using piezoceramic sensors/actuators has taken into account only the stiffness of the piezoceramics but has not considered the damping and the stiffness of the adhesive layer and the piezoceramics at the same time.[8,9] Ignoring damping by the adhesive layer and the piezoceramics leads to discrepancy between measurement and prediction. The dynamics of direct-contact-type sensors and actuators permit a wide frequency range of control. But this method adds mass to the structure so that the structural model needs to be modified to take into account the mass of the sensors and the actuators. In addition to changing the mass, it changes the damping and the stiffness of the structure. To analyze the performance of the controlled structure, the designer should consider the effects of changes in the mass, the damping, and the stiffness by addition of the sensor and the actuator in the structural analysis and the control system design.

The optimum placement for structural vibration control of laminated composite beams with a piezoceramic sensor and actuator bonded on the surface of the beam is investigated numerically and verified experimentally for various fiber orientations. The piezoelectric sensor/actuator is collocated to guarantee stability. Damping and stiffness of the adhesive layer and the piezoceramics are simultaneously taken into account in the finite element formulation. Modal damping $2\zeta\omega$ is chosen as a performance index of structural vibration, whereas most other research has used the damping ratio ζ as the index. The damping ratio represents only a measure of the amplitude decay during one cycle, but the modal damping takes into account the damping ratio as well as the natural frequency. The structural damping index (SDI) is defined from the modal damping. Weights for each vibrational mode are taken into account in the SDI calculation. The optimum location of the sensor/actuator is determined as the point where the SDI is maximum. The effects of the size of the sensor/actuator on the SDI are also investigated.

Method

Laminated composite beams with a piezoceramic sensor/actuator are modeled as two-dimensional plates. Hamilton's principle is used to derive the equation of motion for the plate:

$$\delta \int_{t_1}^{t_2} [T - U + W]\,dt = 0 \tag{1}$$

where T is the kinetic energy, U is the potential energy, and W is the work done by the external forces. The piezoceramic sensor/actuator layers and the adhesive layers are treated as other layers with different material properties in deriving the kinetic and the potential energies.

When the beam is not very thin and not very long, the vibrational response is transmitted dominantly in flexural-type motion, and the vibrational flow in wave-type motion can be ignored. Thus the in-plane displacements can be ignored when only transverse vibration

Received Dec. 16, 1995; revision received May 10, 1996; accepted for publication May 11, 1996.

*Postdoctoral Researcher, Department of Mechanical Engineering.
†Associate Professor, Department of Mechanical Engineering. Member AIAA.
‡Associate Professor, Department of Mechanical Engineering.
§Professor, Department of Mechanical Engineering.

is considered. The displacement vector $\boldsymbol{u}$ and the strain vector ε are expressed as

$$\boldsymbol{u} = \begin{bmatrix} u_x \\ u_y \\ u_z \end{bmatrix} = \begin{bmatrix} -z\dfrac{\partial w}{\partial x} \\ -z\dfrac{\partial w}{\partial y} \\ w \end{bmatrix} = \begin{bmatrix} z\beta_x \\ z\beta_y \\ w \end{bmatrix} \tag{2}$$

$$\varepsilon = \begin{bmatrix} \varepsilon_x \\ \varepsilon_y \\ \gamma_{xy} \end{bmatrix} = \begin{bmatrix} z\dfrac{\partial \beta_x}{\partial x} \\ z\dfrac{\partial \beta_y}{\partial y} \\ z\dfrac{\partial \beta_y}{\partial x} + z\dfrac{\partial \beta_x}{\partial y} \end{bmatrix} = z\boldsymbol{\kappa} \tag{3}$$

where w is the transverse displacement, β_x and β_y are the rotations about the x and y axes, and $\boldsymbol{\kappa}$ is the curvature vector. The kinetic energy T is defined as

$$T = \int_v \frac{1}{2}\rho \dot{\boldsymbol{u}}^T \dot{\boldsymbol{u}}\, dv \tag{4}$$

where ρ is the density and v is the volume of the structure.

The strain energy of the laminated plate is derived from the classic laminated-plate theory.[10] When the potential energy for each layer is summed up in the z direction, the total strain energy becomes

$$U = \frac{1}{2}\int_A \boldsymbol{\kappa}^T D\boldsymbol{\kappa}\, dA \tag{5}$$

where A is the area; D is the flexural stiffness matrix of an anisotropic plate and is expressed as

$$D_{ij} = \frac{1}{3}\sum_{k=1}^{N}(\bar{Q}_{ij})_k\left(z_k^3 - z_{k-1}^3\right) \tag{6}$$

where z_k and z_{k-1} are the distances from the midplane of the laminate to the top and the bottom of the kth lamina.

The work done by external forces is

$$W = \sum_{i=1}^{n_f} \boldsymbol{u}^T(\boldsymbol{x}_i)\boldsymbol{f}(\boldsymbol{x}_i) \tag{7}$$

where $\boldsymbol{f}(\boldsymbol{x}_i)$ is the force vector acting at $\boldsymbol{x}_i$, $\boldsymbol{u}(\boldsymbol{x}_i)$ is the displacement vector at $\boldsymbol{x}_i$, and n_f is the number of forces.

The displacement $\boldsymbol{u}$ and the curvature $\boldsymbol{\kappa}$ are expressed in terms of nodal displacements with the shape functions using a four-node, 12-degree-of-freedom quadrilateral plate-bending element, as follows[11,12]:

$$\boldsymbol{u} = \Psi_u \boldsymbol{q}^e \tag{8}$$

$$\boldsymbol{\kappa} = \Psi_\kappa \boldsymbol{q}^e \tag{9}$$

where Ψ_u and Ψ_κ are the interpolation functions for $\boldsymbol{u}$ and $\boldsymbol{\kappa}$, respectively, and $\boldsymbol{q}^e$ is the element nodal displacement vector. Substitution of energy expressions into Eq. (1) yields the equations of motion for the system in terms of nodal displacements:

$$(M_S + M_B + M_P)\ddot{\boldsymbol{q}} + (K_S + K_B + K_P)\boldsymbol{q} = \boldsymbol{F}_{\text{Ext}} \tag{10}$$

where

$$M_S = \sum_{\text{elem}}\int_{V_S} \Psi_u^T \rho_S \Psi_u\, dv \tag{11a}$$

$$M_B = \sum_{\text{elem}}\int_{V_B} \Psi_u^T \rho_B \Psi_u\, dv \tag{11b}$$

$$M_P = \sum_{\text{elem}}\int_{V_P} \Psi_u^T \rho_P \Psi_u\, dv \tag{11c}$$

$$K_S = \sum_{\text{elem}}\int_{A_S} \Psi_\kappa^T D_S \Psi_\kappa\, dA \tag{11d}$$

$$K_B = \sum_{\text{elem}}\int_{A_B} \Psi_\kappa^T D_B \Psi_\kappa\, dA \tag{11e}$$

$$K_P = \sum_{\text{elem}}\int_{A_P} \Psi_\kappa^T D_P \Psi_\kappa\, dA \tag{11f}$$

$$\boldsymbol{F}_{\text{Ext}} = \sum_{i=1}^{n_f} \Psi_u^T(\boldsymbol{x}_i)\boldsymbol{f}(\boldsymbol{x}_i) \tag{11g}$$

and the subscripts S, B, and P represent the main structure, the adhesive layer, and the piezoceramic materials, respectively.

Damping in the fiber direction is low and damping in the transverse direction is very high because of the characteristics of the polymeric matrix. The damping properties of the composite materials exhibit anisotropic characteristics and can be controlled by changing the fiber orientations and the stacking sequences. We analyze the damping of the laminated composite beams using the concept of specific damping capacity (SDC) suggested by Lin et al.[13] The dampings of the adhesive layer and the piezoceramic sensor/actuator are considered in the system modeling.[14] The SDC φ can be rewritten as

$$\varphi = \frac{\boldsymbol{q}^T K_D \boldsymbol{q}}{\boldsymbol{q}^T(K_S + K_B + K_P)\boldsymbol{q}} \tag{12}$$

where

$$K_D = \sum_{\text{elem}}\int_A \Psi_k^T D^\Delta \Psi_\kappa\, dA \tag{13}$$

and K_D is the damped stiffness matrix. The SDC can be derived for each vibration mode, which is called the modal SDC. When the ith mode shapes are replaced by $\boldsymbol{q}$ in Eq. (12), the ith modal SDC can be obtained. The modal damping matrix $\bar{C}$ can be derived from the modal SDC as

$$\bar{C} = \text{diag}(2\zeta_1\omega_1 \quad 2\zeta_2\omega_2 \quad \cdots \quad 2\zeta_n\omega_n) \tag{14}$$

where

$$2\zeta_i = \varphi_i/2\pi \tag{15}$$

In Eq. (15), $2\zeta_i$ is the damping factor of the ith mode and φ_i is the SDC of the ith mode.

The equation of motion of a structure with multiple degrees of freedom in active contol is expressed in discretized form as

$$M\ddot{\boldsymbol{q}} + C\dot{\boldsymbol{q}} + K\boldsymbol{q} = \boldsymbol{F}_{\text{Ext}} + \boldsymbol{F}_P \tag{16a}$$

where

$$\boldsymbol{F}_P = D_a \boldsymbol{u}_c \tag{16b}$$

and $\boldsymbol{q}(t)$ is the $n \times 1$ displacement vector, $M(=M_S + M_B + M_P)$ is the mass matrix, C is the structural damping, $K(=K_S + K_B + K_P)$ is the stiffness matrix, $\boldsymbol{F}_{\text{Ext}}$ is the external force vector, D_a is the actuator influence matrix, and $\boldsymbol{u}_c$ is the control input to the structure. The $D_a\boldsymbol{u}_c$ are the electromechanical forces generated by the piezoelectric actuator. The initial conditions are

$$\boldsymbol{q}(0) = \boldsymbol{q}_0, \qquad \dot{\boldsymbol{q}}(0) = \dot{\boldsymbol{q}}_0$$

We introduce the modal coordinate transformation as follows:

$$\boldsymbol{q}(t) = \Phi\eta(t) \tag{17}$$

where Φ is the open-loop modal matrix obtained by solving the eigenvalue problem associated with the nominal mass and stiffness matrices and $\eta(t)$ is the $n \times 1$ vector of modal coordinates.

The transformed equation of motion becomes

$$\bar{M}\ddot{\eta} + \bar{C}\dot{\eta} + \bar{K}\eta = \bar{F}_{\text{Ext}} + \bar{D}u_c \tag{18}$$

where the transformed modal space mass, damping, stiffness, external forces, and control influence matrices are, respectively, given by

$$\bar{M} = \Phi^T M \Phi = I \tag{19a}$$

$$\bar{C} = \Phi^T C \Phi = \text{diag}(2\zeta_1\omega_1, 2\zeta_2\omega_2, \ldots, 2\zeta_n\omega_n) \tag{19b}$$

$$\bar{K} = \Phi^T K \Phi = \text{diag}(\omega_1^2, \omega_2^2, \ldots, \omega_n^2) \tag{19c}$$

$$\bar{F}_{\text{Ext}} = \Phi^T F_{\text{Ext}} \tag{19d}$$

$$\bar{D} = \Phi^T D_a \tag{19e}$$

The first-order state–space form of the system equations equivalent to Eq. (18) is

$$\dot{x} = Ax + Bu_c + B_0 \tag{20}$$

where

$$A = \begin{bmatrix} 0 & I \\ -\bar{K} & -\bar{C} \end{bmatrix}, \qquad B = \begin{bmatrix} 0 \\ \bar{D} \end{bmatrix}$$

$$B_0 = \begin{bmatrix} 0 \\ \bar{F}_{\text{Ext}} \end{bmatrix}, \qquad x = \begin{bmatrix} \eta \\ \dot{\eta} \end{bmatrix}$$

In Eq. (20), the state vector $x(t) \in R^{2n}$, control vector $u_c(t) \in R^m$, and the system matrix A and the control influence matrix B may contain time-varying elements. The control input with feedback gain of $G(t)$ is

$$u_c = -Gx \tag{21}$$

When the piezoceramic sensor picks up the strain rate of the structure, the actuator functions to increase the modal damping ($\bar{C}$) of the system matrix A in Eq. (20). That is, the structural vibration control using the piezoceramic sensor/actuator increases the damping of the structure. Total modal damping of the structure is composed of inherent modal damping, $\bar{C}$, and active modal damping, $\bar{C}_a$, actuated by the control input. Inherent damping means the damping of the structure with no control input, namely, passive damping. From the viewpoint of structural control, inherent damping is very important for vibration control as well as for free vibration. If the inherent damping of each vibration mode is large, the same control performance can be achieved using smaller control efforts.

The SDI is defined by taking into account the modal damping and the contribution of each vibrational mode. The expansion theorem is used to determine the weighting factor of each mode to the total response of the structure, because the displacement in structural vibration can be expressed as the superposition of every vibrational mode. The given initial displacement q_0 can be expressed as

$$q_0 = \sum_{r=1}^{N} c_r \phi_r \tag{22}$$

In Eq. (22), c_r is the weighting factor for each mode, N is the number of lower modes that is taken into account, and ϕ_r is the mode shape. The SDI is defined as

$$\text{SDI} = \sum_r 2\zeta_r \omega_r c_r \tag{23}$$

Six lower modes are considered in this investigation. The optimum location of the sensor/actuator is chosen at the point of maximum SDI value.

Results and Discussion

Optimum placement of the piezoelectric sensor and actuator for vibration control of the carbon–epoxy laminated composite beams is investigated with stacking sequences of $[\theta_4/0_2/90_2]_s$, where $\theta = 0$, 15, 30, 45, 60, 75, and 90 deg. The beam specimen is made of carbon prepreg (CU125NS). The direction of the beam length is chosen as 0 deg of fiber orientation. The thickness of the carbon prepreg is 0.125 mm, and the size of the specimen is 230 × 20 × 2 mm.

Table 1 Mechanical properties of carbon–epoxy laminates (CU125NS)

Property	Symbol	Value
Young's modulus in fiber direction	E_1	114.7×10^9 Pa
Young's modulus in transverse direction	E_2	7.589×10^9 Pa
Shear modulus	G_{12}	4.77×10^9 Pa
Poisson ratio	ν_{12}	0.28
Volume density	ρ	1510 kg/m^3
Damping capacity in fiber direction	φ_{S1}	0.013966
Damping capacity in transverse direction	φ_{S2}	0.049120
Damping capacity in shear direction	φ_{S12}	0.074344

Table 2 Mechanical properties of piezoceramics

Property	Symbol	Value
Piezoelectric constants	d_{31}	-260×10^{-12}C/N
	d_{33}	540×10^{-12}C/N
	d_{15}	750×10^{-12}C/N
Piezoelectric voltage constants	e_{31}	-8.7×10^{-3} m^2/C
Relative dielectric constants	$\varepsilon_{11}/\varepsilon_0$[a]	3100
	$\varepsilon_{33}/\varepsilon_0$	3400
Young's modulus	E_{11}	59×10^9 Pa
	E_{33}	52×10^9 Pa
	E_{55}	21×10^9 Pa
Damping capacity	φ_{P1}	0.0748644
	φ_{P2}	0.0748644
Damping capacity in shear direction	φ_{P12}	0.1061625

[a] ε_0 is the permittivity of free space [$=1/(36\pi \times 10^9)$ F m^{-1}].

Table 3 Mechanical properties of adhesive layer

Property	Symbol	Value
Young's modulus	E_B	1.78×10^9 Pa
Volume density	ρ_B	1050 kg/m^3
Poisson ratio	ν_{B12}	0.3
Damping capacity	φ_{B1}	0.049120
	φ_{B2}	0.049120
Damping capacity in shear direction	φ_{B12}	0.049120

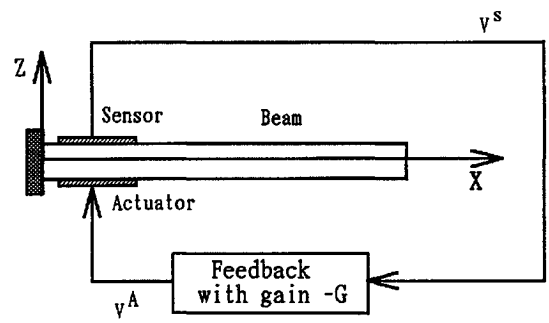

Fig. 1 Beam with piezoceramic sensor/actuator.

Table 1 shows the mechanical properties of the carbon–epoxy laminates. The damping properties φ_{S1}, φ_{S2}, and φ_{S12} are measured using the impulse technique. The finite element method is utilized to model the system, and the finite element model of the beam consists of 46 elements with 72 nodes. The modal coordinate transformation is introduced and the dynamic characteristics of the lower six modes in the composite beams are analyzed. The beam with the piezoceramic sensor/actuator is shown in Fig. 1. The width and the thickness of the piezoceramics in Fig. 1 are 20 and 0.5 mm, respectively. The basic mechanical properties of the piezoceramics are summarized in Table 2 (Ref. 15). The adhesive material used to attach the piezoceramic sensor/actuator to the beam is cyanoacrylate adhesive.[16] The material properties of the adhesive layer are summarized in Table 3. The measured thickness of the adhesive layer is 0.05 ± 0.01 mm. The damping capacity of the adhesive layer can be thought of as isotropic.

Table 4 Effects of piezoceramic sensor/actuator on the dynamics of the entire structure

Mode n	Case 1[a]		Case 2[b]	
	ζ_n	f_n	ζ_n	f_n
1	0.001113	52.875	0.002284	66.315
2	0.001113	332.09	0.002138	373.54
3	0.005565	412.87	0.005671	523.06

[a]No piezoceramics are bonded.
[b]Piezoceramics are bonded on the specimen.

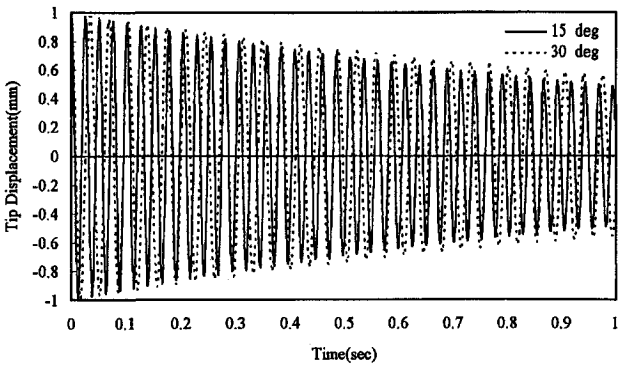

Fig. 2 Time history of free vibrations.

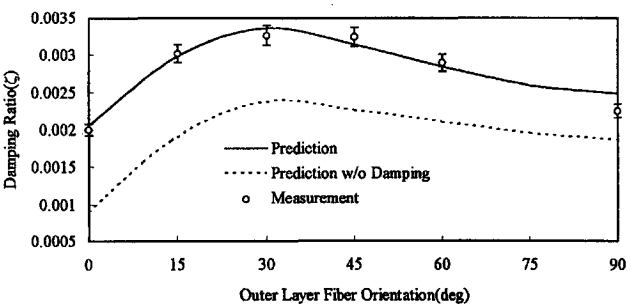

Fig. 3 Damping ratio vs outer-layer fiber orientation with lead zirconate titanate (PZT).

The damping and the stiffness of the beams are controlled by changing the fiber orientation in the outer layer. Figure 2 shows free vibrations of the $[15_4/0_2/90_2]_s$ specimen and the $[30_4/0_2/90_2]_s$ specimen without piezoceramics. In Fig. 2, the amplitude at the tip of the $[15_4/0_2/90_2]_s$ specimen decayed faster than that of the $[30_4/0_2/90_2]_s$ specimen by 13.0% when the vibrational amplitude was measured after 1 s, although the damping ratio ζ of the former is smaller than that of the latter by 10.6%. From this, it can be said that modal damping is a more appropriate parameter of vibration suppression performance.

Attaching piezoceramics to the structure as a sensor and an actuator changes structural parameters such as mass, damping, and stiffness of the main structure. Table 4 shows the effects of the piezoceramic sensor/actuator on the dynamics of the entire structure in the case of the $[0_4/0_2/90_2]_s$ beam with and without a piezoceramic sensor/actuator whose length is 50 mm. The damping ratio and the natural frequency of each vibrational mode change as the piezoceramic sensor/actuator is attached to the beam. Measurements of the damping ratio, the fundamental frequency, and the modal damping of the first bending mode are carried out using the impulse technique to verify the validity of the finite element formulation. Figure 3 shows the damping ratio of the beams with the piezoceramics whose length is 50 mm and whose center is 35 mm away from the clamping side of the beam. The damping ratio of the beam with piezoceramics is maximum at fiber orientation of $[30_4/0_2/90_2]_s$ and minimum at fiber orientation of $[0_4/0_2/90_2]_s$. In Fig. 3, the predicted damping ratios, with which we have taken into account both the damping and the stiffness of the adhesive layer and the piezoceramics, are in good agreement with the measured values. However, the prediction

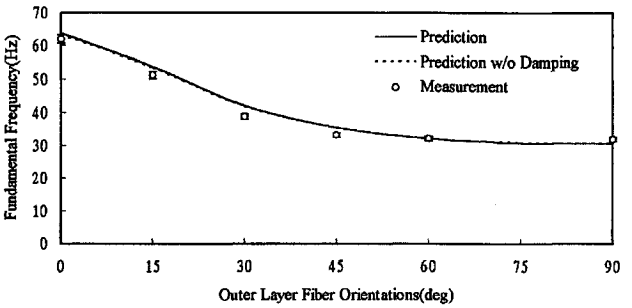

Fig. 4 Fundamental frequency vs outer-layer fiber orientation with PZT.

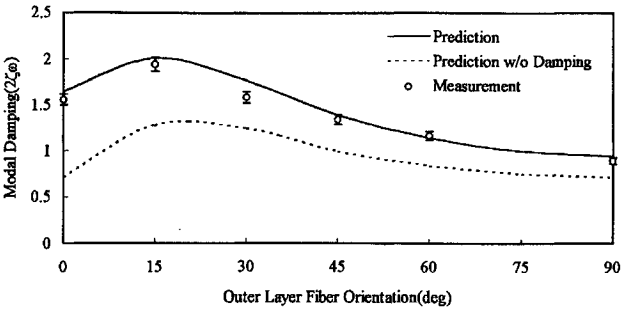

Fig. 5 Modal damping with PZT.

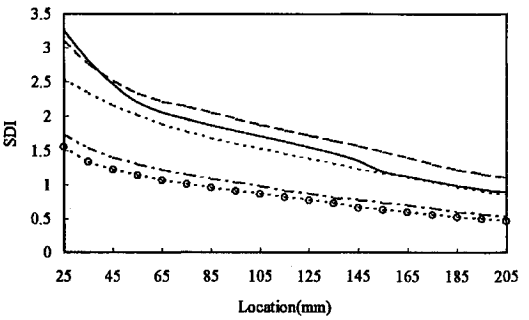

Fig. 6 SDI for various outer-layer fiber orientations (sensor/actuator length = 50 mm): ——, 0 deg; – – –, 15 deg; - - - -, 30 deg; – - – -, 60 deg; and o, 90 deg.

without damping, in which the damping and the stiffness of the adhesive layer and the damping of the piezoceramics are ignored, shows a large discrepancy between the prediction and the measurement. The predicted values are connected with a line smothly. Figure 4 shows the fundamental frequency of the beams with piezoceramics. From these data, one can realize that the stiffness of the adhesive layer does not affect the total structure very much. Figure 5 shows the modal damping $2\zeta\omega$ of the first bending mode of the beams with the piezoceramics. The measured modal damping agrees very well with the predicted value when the damping and the stiffness of the adhesive layer and the piezoceramics are taken into account. A significant discrepancy also occurs when the damping and the stiffness of the adhesive layer and the damping of the piezoceramics are ignored in the system modeling (prediction without damping).

The SDI depends on the location of the sensor/actuator for a fixed length of the piezoceramics. The SDI for various outer-layer fiber orientations of the beams is plotted in Fig. 6. The sensor/actuator is collocated and its length is 50 mm. The SDI is very sensitive to the location of sensor/actuator and the fiber orientations. A beam with higher stiffness is more sensitive to the sensor/actuator location than a beam with lower stiffness. The $[0_4/0_2/90_2]_s$ specimen has higher SDI than the $[15_4/0_2/90_2]_s$ specimen when the sensor/actuator lies closer to the clamping side of the beam. But as the position of the sensor/actuator moves farther away from the clamping side of the beam, the $[15_4/0_2/90_2]_s$ specimen shows a higher SDI than

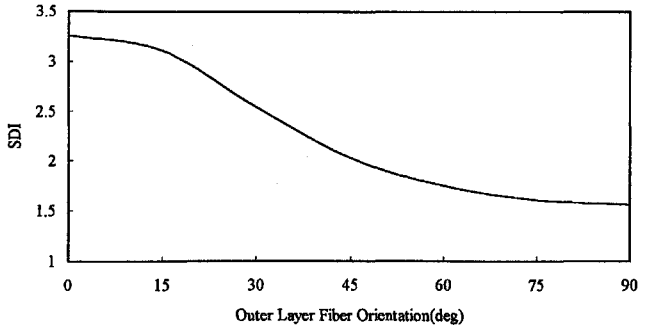

Fig. 7 SDI for optimal locations (sensor/actuator length = 50 mm).

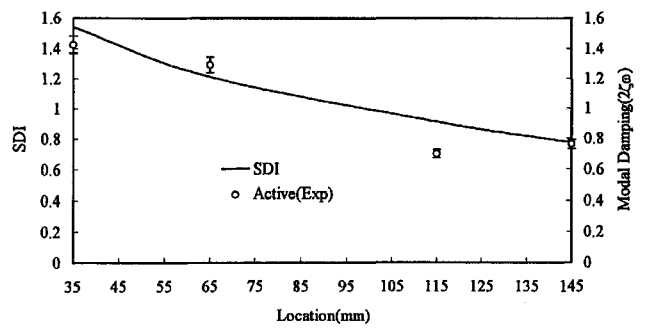

Fig. 8 Experiment on locations (sensor/actuator length = 50 mm).

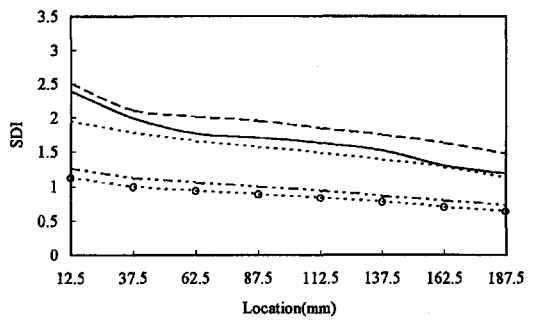

Fig. 9 SDI for various outer-layer fiber orientations (sensor/actuator length = 25 mm): ——, 0 deg; – – –, 15 deg; - - - -, 30 deg; – - – -, 60 deg; and o, 90 deg.

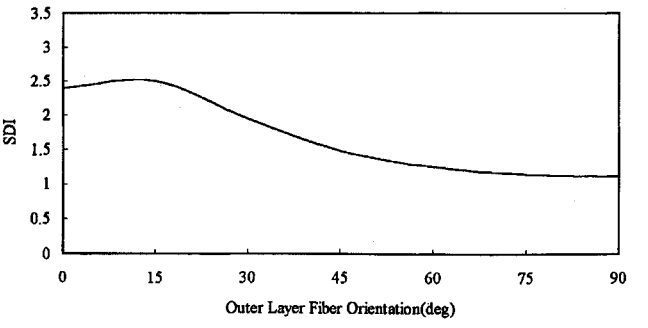

Fig. 10 SDI for optimal locations (sensor/actuator length = 25 mm).

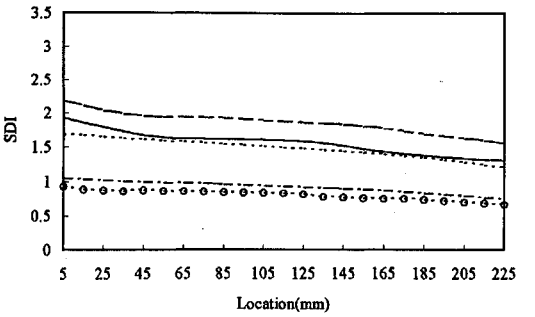

Fig. 11 SDI for various outer-layer fiber orientations (sensor/actuator length = 10 mm): ——, 0 deg; – – –, 15 deg; - - - -, 30 deg; – - – -, 60 deg; and o, 90 deg.

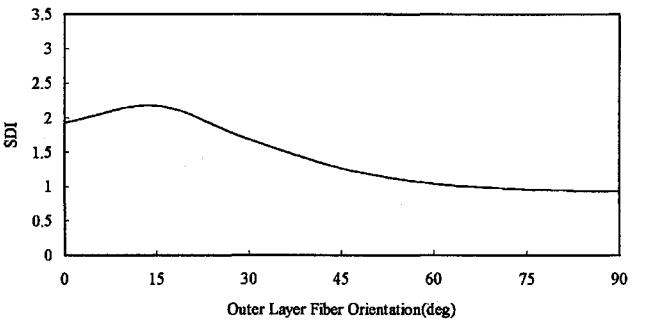

Fig. 12 SDI for optimal locations (sensor/actuator length = 10 mm).

the $[0_4/0_2/90_2]_s$ specimen. Figure 7 shows the SDI for optimum locations of a 50-mm-long sensor/actuator. The $[0_4/0_2/90_2]_s$ specimen has the maximum SDI for the optimum location. It can be said that a beam with higher stiffness works better than a flexible beam. The experimental results of the $[60_4/0_2/90_2]_s$ specimen at the sensor/actuator locations are shown in Fig. 8. The active modal damping of the first bending mode is measured because the first bending mode is dominant in the beam vibration. Experimentally measured active modal damping values agree with the calculated SDI values.

The size of the piezoelectric sensor/actuator also can affect the SDI. Figure 9 shows the SDI for various outer-layer fiber orientations of the beams with a 25-mm-long piezoelectric sensor/actuator. The $[15_4/0_2/90_2]_s$ specimen has a higher SDI than any other fiber orientation beam for all locations. The beam with higher stiffness is more sensitive to the locations of the sensor/actuator. Figure 10 shows the SDI for optimum locations of the 25-mm-long sensor/actuator. The $[15_4/0_2/90_2]_s$ specimen has the maximum SDI for the optimum locations. Figure 11 shows the SDI for various outer-layer fiber orientations of the beams with the piezoelectric sensor/actuator of 10-mm length. Again, the $[15_4/0_2/90_2]_s$ specimen has higher SDI than any other specimen for all locations, and a beam with higher stiffness is more sensitive to the locations of the sensor/actuator. Figure 12 shows the SDI for optimum locations of the 10-mm-long sensor/actuator. The $[15_4/0_2/90_2]_s$ specimen has the maximum SDI for the optimum locations.

Conclusions

The optimum placement of the collocated piezoelectric sensor/actuator for controlling vibration of laminated composite beams is investigated numerically and verified experimentally. The finite element method is used to predict the structural characteristics of the laminated composite beams. The following conclusions have been drawn.

A systematic and quantitative method for the optimum placement of the sensor/actuator is proposed for the vibration control of the laminated composite beam. The SDI, which has taken into account the modal damping and the contribution of each vibrational mode, is a good criterion for determining the optimum location of the sensor/actuator because it is based on the inherent damping of the structure.

The numerical simulation and the experimental results show that the SDI depends on the stiffness of the host structure, the location of the sensor/actuator, and the size of the sensor/actuator.

The modal damping $2\zeta\omega$ is a more appropriate performance index of vibration suppression than the damping ratio ζ, from the viewpoint of structural control. The damping ratio represents only the amplitude decay during one cycle, but modal damping takes into account both the amplitude decay and the settling time.

Acknowledgment

The support of the Agency for Defense Development under Project No. ADD-93-5-4 is gratefully acknowledged.

References

[1]Hamdan, A. M. A., and Nayfeh, A. H., "Measures of Modal Controllability and Observability for First- and Second-Order Linear Systems," *Journal of Guidance, Control, and Dynamics*, Vol. 12, No. 3, 1989, pp. 421–428.

[2]Kim, Y., and Junkins, J. L., "Measure of Controllability for Actuator Placement," *Journal of Guidance, Control, and Dynamics*, Vol. 14, No. 5, 1991, pp. 895–902.

[3]Crawley, E. F., and Javier de Luis, "Use of Piezoelectric Actuators as Elements of Intelligent Structures," *AIAA Journal*, Vol. 25, No. 10, 1987, pp. 1373–1385.

[4]Devasia, S., Meressi, T., Paden, B., and Bayo, E., "Piezoelectric Actuator Design for Vibration Suppression: Placement and Sizing," *Journal of Guidance, Control, and Dynamics*, Vol. 16, No. 5, 1993, pp. 859–864.

[5]Kirby, G. C., Matic, P., and Lindner, D. K., "Optimal Actuator Size and Location using Genetic Algorithms for Multivariable Control," *Adaptive Structures and Composite Materials: Analysis and Application*, edited by E. Garcia, AD-Vol. 45/MD-Vol. 54, American Society of Mechanical Engineers, New York, 1994, pp. 325–335.

[6]Main, J. A., Garcia, E., and Howard, D., "Optimal Placement and Sizing of paired Piezoactuators in Beams and Plates," *Smart Materials and Structures*, Vol. 3, No. 3, 1994, pp. 373–381.

[7]Wang, B. T., Burdisso, R. A., and Fuller, C. R., "Optimal Placement of Piezoelectric Actuators for Active Structural Acoustic Control," *Journal of Intelligent Material Systems and Structures*, Vol. 5, No. 1, 1994, pp. 67–77.

[8]Detwiler, D. T., and Shen, M. H., "Two-Dimensional Finite Element Analysis of Laminated Composite Plates Containing Distributed Piezoelectric Actuators and Sensors," *A Collection of Technical Papers of the AIAA/ASME Adaptive Structures Forum*, AIAA, Washington, DC, 1994, pp. 451–460.

[9]Ha, S. K., Keilers, C., and Chang, F. K., "Finite Element Analysis of Composite Structures Containing Distributed Piezoceramic Sensor and Actuators," *AIAA Journal*, Vol. 30, No. 3, 1992, pp. 772–780.

[10]Hwang, W. S., and Park, H. C., "Finite Element Modeling of Piezoelectric Sensors and Actuators," *AIAA Journal*, Vol. 31, No. 5, 1993, pp. 930–937.

[11]Batoz, J. L., and Tahar, M. B., "Evaluation of a New Quadrilateral Thin Plate Bending Element," *International Journal of Numerical Methods in Engineering*, Vol. 18, 1982, pp. 1655–1677.

[12]Becker, E. B., Carey, G. F., and Oden, J. T., *Finite Elements*, Prentice–Hall, Englewood Cliffs, NJ, 1981, pp. 194–199.

[13]Lin, D. X., Ni, R. G., and Adams, R. D., "Prediction and Measurement of the Vibrational Damping Parameters of Carbon and Glass Fibre-Reinforced Plastic Plates," *Journal of Composite Materials*, Vol. 18, March 1984, pp. 132–152.

[14]Kang, Y. K., Park, H. C., Hwang, W., and Han, K. S., "Prediction and Measurement of Modal Damping of Laminated Composite Beams with Piezoceramic Sensor/Actuator," *Journal of Intelligent Material Systems and Structures*, Vol. 7, No. 1, 1996, pp. 25–32.

[15]Anon., *Piezoelectric Ceramics*, Fuji Ceramics Co., Ltd., 1994.

[16]Lee, J. K., and Marcus, M. A., "The Deflection-Bandwidth of Poly(vinylidense Fluoride) Benders and Related Structures," *Ferroelectrics*, Vol. 32, No. 1/4, 1981, pp. 93–101.